

Initial Tests of a Lightweight, Self-Excited MHD Power Generator

C. D. Maxwell* and S. T. Demetriades†
 STD Research Corporation, Arcadia, California

Data from the first seven power tests of a lightweight, self-excited MHD generator system are presented. Among the achievements of these tests were: 1) highest power from a diagonally connected MHD generator in the United States (4.8 MW, gross), 2) fastest self-excitation time for an MHD generator (0.4 s), and 3) highest specific power for a combustion-driven MHD generator in the United States on the basis of gross or net power per unit system mass. The tests show evidence of strong MHD interaction processes, including magnetoaerothermal effects, as expected from the design calculations. Solution of the intricate problems presented by these processes for each size of this family of MHD generators is necessary before the ultimate performance of these systems is realized. The software for obtaining these solutions has been validated, and some results are discussed in this paper.

Nomenclature

A_G	= MHD generator cross-sectional area, m^2
D_G	= MHD generator mean diameter, m
g	= conductivity nonuniformity factor, $\langle \sigma \rangle \langle 1/\sigma \rangle$
G	= plasma nonuniformity factor, $g + (g-1)\beta^2$
L	= magnet inductance, H
R_J	= MHD generator internal impedance, Ω
R_L	= load resistance, Ω
R_M	= magnet resistance, Ω
R_{etc}	= other circuit resistances, Ω
R^*	= (open-circuit voltage)/(magnet current)
X_G	= MHD generator active length, m
β	= Hall parameter
σ	= electrical conductivity, S/m
τ^*	= self excitation time constant
θ	= diagonalization angle, measured from direction perpendicular to flow and magnetic field

Introduction

THE production of net electrical energy by an MHD generator requires either very large equipment,¹ or use of a cryogenic magnet,² or high electrical conductivity plasmas.³ For MHD generator applications requiring portability, ruggedness, and self-containment in remote locations, the last option has many practical advantages. Among the MHD generators that have produced net energy, the Pamir-I obtained the highest conductivity, approximately 50 S/m, by using metalized solid propellants.³

Hybrid propellants (solid fuel, gaseous, or liquid oxidizer) have been promising candidates for achieving high-conductivity MHD working fluids for many years.⁴ Tests at STD Research Corporation in 1981-1982 demonstrated electrical conductivities in excess of 100 S/m in the seeded combustion products from a subscale hybrid rocket combustor.

Such conductivities made possible the design of a family of lightweight, self-excited MHD generators with relatively low-field, conventional air-core magnets. A small STD/MHD generator (Fig. 1) was constructed in 1982-83, and testing began in 1983. Self-excitation was demonstrated in May 1983, on the third power test. Sustained net electrical

power production was demonstrated in August 1984 on the fourth power test, 84-001, shown in Fig. 2. In August 1984, a peak power of 4.8 MW was achieved on the seventh and most recent power test. Figure 3 summarizes the power test history.

Among the novel features of the STD/MHD generator design was the selection of a single-load diagonal electrical configuration for the self-excited MHD generator. Many of the advantages of the diagonal configuration for self-excitation have been recognized in the recent Soviet literature.^{5,6} An important advantage demonstrated in these tests is the potentially superior excitation speed relative to the continuous electrode Faraday configuration.

The self-excited generator is a high-interaction device, because it is primarily the reduction of flow speed by the MHD interaction that limits the self-excitation process. Despite the conservatism of the initial generator design and the modest specific energy extraction achieved thus far (0.25 MJ/kg), it is clear that magnetoaerothermal effects⁷ and other strong MHD interaction processes are very important in the present device, as they have been in previous self-excited generator tests.³

Generator Characteristics

A simplified electrical schematic of the generator configuration tested to date is presented in Fig. 4. The nominal component characteristics shown in Fig. 4 vary somewhat with ambient temperature and other factors.

In a typical test sequence, the switch S1 is closed a few seconds before combustor ignition to provide an initial magnetic field of 0.45 T. (The minimum field to initiate self-excitation has not been determined yet.) After ignition, the generator voltage rises. When it exceeds the battery open-circuit voltage, the diode D1 removes the battery from the circuit, and the generator self-excites. In the last two power tests, switch S2 was closed during the self-excitation phase to achieve maximum speed and magnetic field and then opened to power the load. At the end of a power pulse, the oxidizer flow is stopped, the generator impedance rises, and the magnet discharges through the diode D2.

The 60-deg (from vertical) diagonal, heat-sink generator channel is constructed of graphite frames insulated by castable ceramic. The pressure case is filament-wound in a manner similar to that suggested in Ref. 8. The generator active region is 1.27 m long and has an area ratio of 2.27. The generator is designed for a nominal mass flow rate of 20

Received Nov. 13, 1985; revision received April 14, 1986. Copyright © 1986 by STD Research Corporation. Published by the American Institute of Aeronautics and Astronautics, Inc., with permission.

*Vice President. Member AIAA.

†President and Technical Director. Fellow AIAA.

kg/s. The system is designed to self-excite when the plasma conductivity exceeds 50 S/m.

The mass of the entire system, excluding the batteries (which are greatly overspecified at 800 kg) with 30 s of propellant, does not exceed 6000 kg, of which the magnet coils comprise approximately two-thirds. The system is not optimized for weight. It is mounted on a 9-m-long trailer and is towed to the isolated test site by a pickup truck.

Test Results

Primary data from the two tests with the highest power output, tests 84-002 and 84-004, are presented in Figs. 5 and 7, respectively. The format follows the practice established by Demetriades some time ago⁹ of presenting a simultaneous and continuous record of all primary measurements. The following narrative describes the events in these two tests.

Test 84-002

A 22-m Ω load was in series with the generator throughout the test. (The switch S2 was not present.) Figure 5 shows that the self-excitation time was approximately 0.5 s based on the 10-90% rise time of the current. Because the magnet resistance is nearly the same as the load resistance in this test, the net MHD power is approximately half the gross power shown in Fig. 6. The MHD power is about 30 times higher than the power from the initiation battery. The maximum MHD power of 3.9 MW occurred during self-excitation. The steady-state power was approximately 3.4 \pm 0.3 MW.

In test 84-002, significant erosion was observed on the diffuser surface receiving flow from the middle of the anode wall ("anodes" receive electrons from the plasma). No visible erosion was found on the generator electrode surfaces.

Test 84-004

The switch S2 was closed to short out a 67-m Ω load until the time 11.4 s, as indicated by the jump in generator voltage

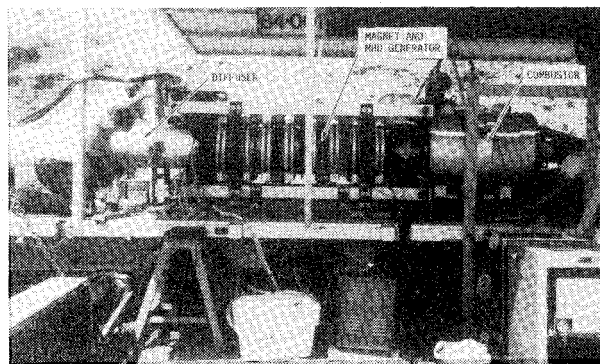


Fig. 1 Self-excited MHD generator equipment.

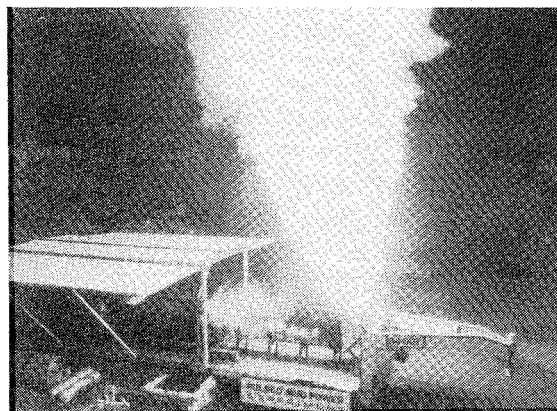


Fig. 2 Self-excited MHD generator during test 84-001.

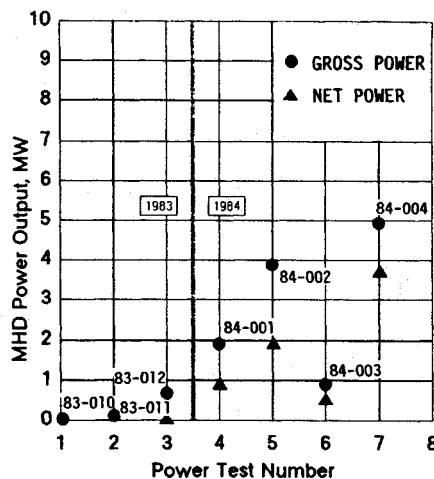


Fig. 3 Peak MHD power levels achieved in the first seven power tests of the STD/MHD pulse power system. Gross power is the product of MHD generator terminal voltage and current. Net power is the difference between gross power and the I^2R power dissipated in the magnet.

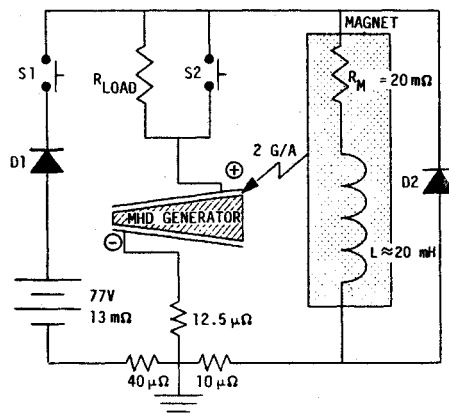


Fig. 4 Simplified schematic of the electrical circuit for the self-excited MHD generator.

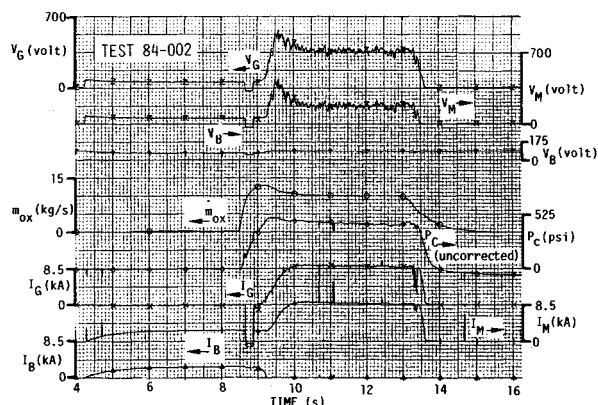


Fig. 5 Variation of measured quantities during test 84-002. V_G =generator terminal voltage, V_M =voltage across magnet, V_B =voltage across excitation battery, \dot{m}_{ox} =flow rate of oxidizer, P_c =combustion chamber pressure, uncorrected for transducer drift, I_G =total current through battery. Times are relative to the test sequence start. The step at 8.65 s is an artifact of the data acquisition system.

at that time in Fig. 7. The self-excitation time was approximately 0.4 s. The peak power of 4.8 MW occurred during the self-excitation process, as shown in Fig. 8. This corresponds to an average power density of approximately 100 MW/m³ and a specific power based on loaded system mass of approximately 0.8 kW/kg. When the switch S2 opened, the channel power increased from about 2.7 to 3.7 MW, due to improved generator loading.

At the 11.8-s point in test 84-004, diffuser erosion of the type observed in test 84-002 caused a gas leak on the mid-anode side of the diffuser. An electrical short developed through the gas leak to the grounded trailer body, causing superficial damage to the trailer. Again, there was no apparent effect on the generator interior surfaces or on the remainder of the system.

"Electrotechnical" Parameters

Velikhov³ provides a useful summary of the circuit parameters, or "electrotechnical" parameters, of the self-excited generator, with emphasis on the continuous electrode Faraday generator. These ideas are easily extended to a diagonal generator configuration. An examination of some of these parameters for the present device reveals some of the tradeoffs between the two configurations.

We write the excitation time constant of either electrical configuration as

$$\tau^* = L / [R^* - (R_G + R_M + R_L + R_{etc})] \quad (1)$$

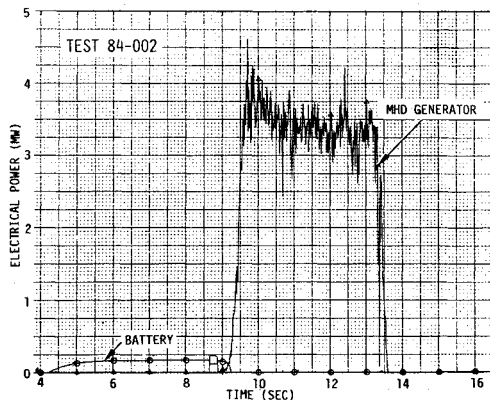


Fig. 6 Variation of the gross electrical power produced by the excitation battery and the MHD generator in test 84-002, based on the currents and voltages shown in Fig. 5.

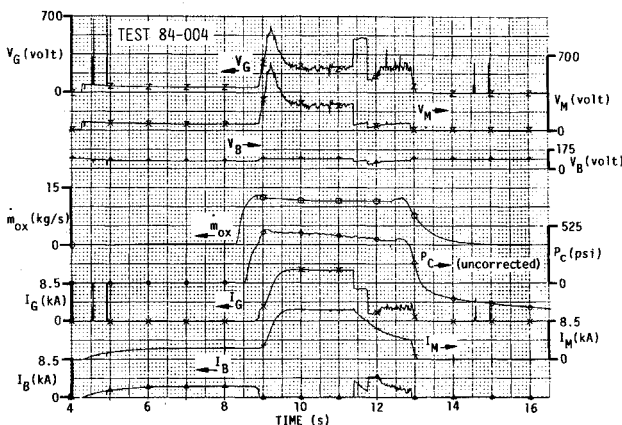


Fig. 7 Variation of measured quantities during test 84-004. (See Fig. 5 for symbol definitions.) The discrete events at the end of the test are 1) the opening of the switch S2 at 11.4 s and 2) gas-leak-initiated diffuser-to-ground short at 11.75 s.

where L is the magnet inductance and the subscripts G , M , L , etc., denote, respectively, the resistance (internal impedance) of the MHD generator, the magnet, the load, and any other resistance in series with the generator and magnet. The quantity R^* is the ratio of the generator open-circuit voltage at a given magnetic field to the current required from the generator to produce that magnetic field.

One purpose of the load switch S2 is to determine the generator parameters R^* and R_G . If the generator voltage/current characteristics are examined immediately before and after the switch is opened, we obtain an instantaneous load line at essentially constant magnetic field. Load line information is not easy to extract from the self-excitation phase because the magnetic field is changing on the same time scale as the impedance. With the switch, the load changes in less than a millisecond, the flow stabilizes in a few milliseconds, but the magnetic field responds on the order of hundreds of milliseconds. The 0.3-ms data rate permits these events to be resolved by the data acquisition system.

The load line thus obtained for test 84-004 is shown in Fig. 9. R_G is the slope of the load line, while R^* is the ratio of the open-circuit voltage to the magnet current just before the switch is opened. We find an open-circuit voltage of 1040 V and an internal impedance of 73 m Ω . These values correspond to a magnet current of approximately 11.2 kA, giving $R^* = 93$ m Ω . These values are self-consistent. Before the load switch, the denominator of Eq. (1) contains only R^* , R_G ,

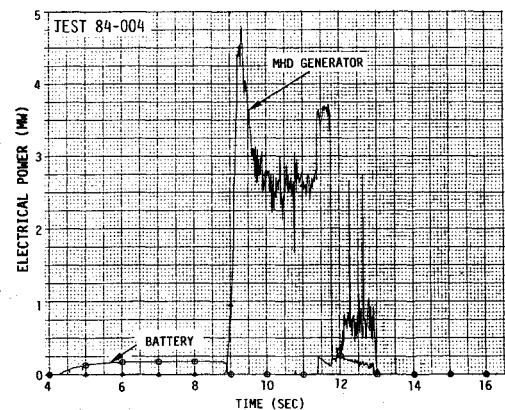


Fig. 8 Variation of gross electrical power produced by the excitation battery and the MHD generator in test 84-004, based on currents and voltages in Fig. 7.

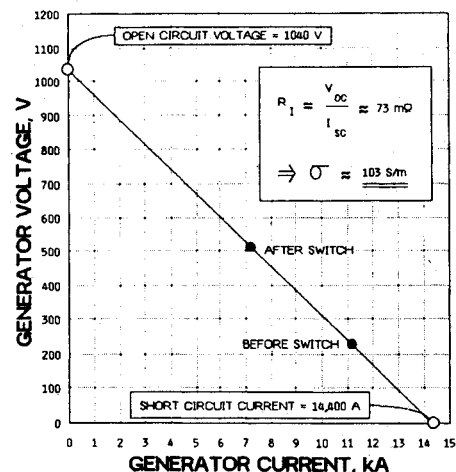


Fig. 9 The instantaneous voltage/current characteristic during test 84-004, as determined by measurements immediately before and after a 67-m Ω load was switched into the generator/magnet circuit. (See electrical schematic, Fig. 4.)

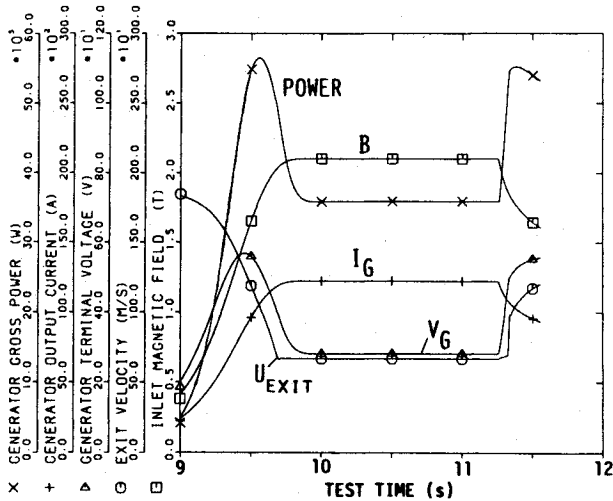


Fig. 10 Quasi-one-dimensional TRANSIENT simulation of test 84-004.

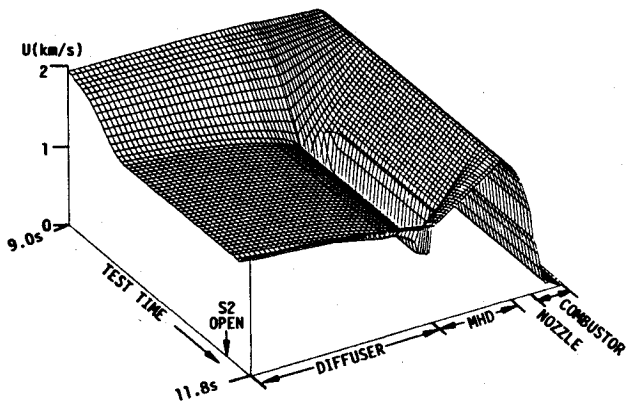


Fig. 11 Flowfield evolution in the quasi-one-dimensional simulation of test 84-004.

and $R_M = 20 \text{ m}\Omega$, the sum of which is zero, implying an infinite excitation time, i.e., steady state.

The value of R^* during self-excitation is higher than $93 \text{ m}\Omega$. R^* varies with the velocity of the flow.³ We have carried out simulations of the events of test 84-004 using the STD/MHD TRANSIENT family of codes with the quasi-one-dimensional approximation, as described in Ref. 10. Typical results are shown in Figs. 10 and 11. Figure 10 shows that the exit velocity drops by more than a factor of 2 in the simulation of the self-excitation process. As seen in Fig. 11, a shock is predicted to stand near the exit of the generator, followed by a reacceleration of the flow in the diffuser. The value of R^* in the simulation decreases by 20% as the generator self-excites.

It may be shown in a "zero-dimensional" analysis that the ratio of values for R^* for the diagonal generator to the continuous electrode Faraday generator is, for uniform plasma early in self-excitation ($\beta \rightarrow 0$):

$$R^*(\text{Diag})/R^*(\text{C.Far.}) \sim (X_G/D_G)\tan\theta/(1+\tan^2\theta) \quad (2)$$

where X_G , D_G , and θ are the length, diameter, and diagonalization angle of the generator, respectively. The denominator of Eq. (1) can thus be potentially larger for a diagonal generator, giving shorter excitation times, if the circuit resistances can be made small. It is noted that the ratio in Eq. (2) is maximized for $\theta = 45 \text{ deg}$; however, electrical conversion efficiency demands higher angles when the Hall

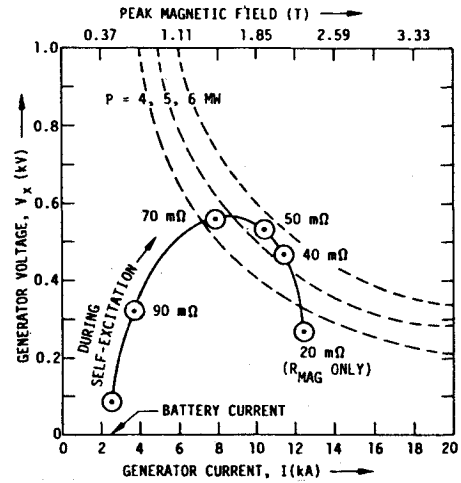


Fig. 12 The steady-state voltage/current characteristics of the MHD generator from quasi-one-dimensional simulations of the test 84-004 conditions. The generator load is the sum of the load and magnet impedances.

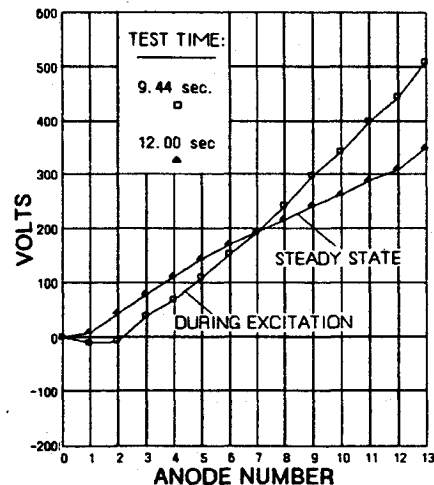


Fig. 13 Measured variation of anode voltage to ground during excitation phase and at steady state during test 84-002. Anodes and frames are numbered sequentially from upstream to downstream. Anode no. 0 is grounded.

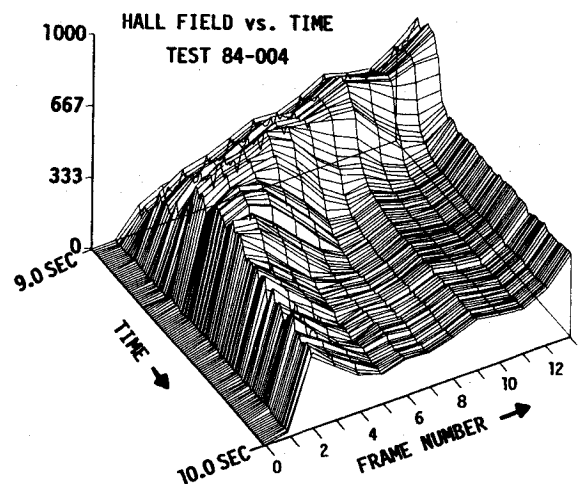


Fig. 14 Measured evolution of the Hall field distribution during self-excitation in test 84-004.

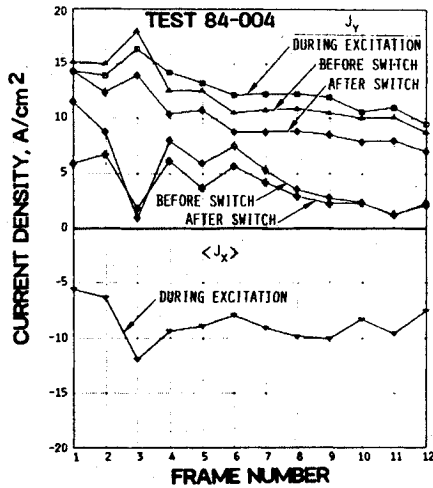


Fig. 15 Variation of the distribution of normal and axial current density during test 84-004. Data are derived from measurements of anode-to-cathode voltage differences in each frame: during excitation, 9.20 s; before switch, 11.25 s; after switch, 11.67 s.

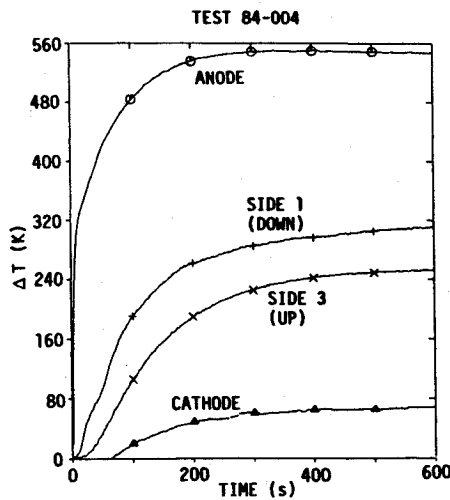


Fig. 16 Temperature increase above ambient measured on all four sides of MHD channel at outer layer of ceramic, 20 in. from inlet.

parameter is low,¹¹ as it is in the present device. The ratio of the internal impedances is approximately

$$R_G(\text{Diag})/R_G(\text{C.Far}) \sim (X_G/D_G)^2/(1 + \tan^2\theta) \quad (3)$$

so that high plasma conductivity is important to minimize internal impedance and reap the benefit of larger R^* in a diagonal machine.

The generator internal impedance can be used to estimate the electrical conductivity without the need for an estimate of velocity, which was not accurately measured. The "zero-dimensional" formula for conductivity in terms of diagonal generator internal impedance may be written as

$$\begin{aligned} \langle \sigma \rangle &= \frac{(X_G/A_G)(1 + \beta^2)(g)}{R_G(G + \tan^2\theta)} \\ &= \frac{(1.27/0.050)(1 + 0.16)(1.03)}{(0.073)(1.035 + 3)} \\ &= 103 \text{ S/m} \end{aligned} \quad (4)$$

where the Hall parameter β is a lower limit taken from simulations, and the conductivity nonuniformity factor

$g = \langle \sigma \rangle / \langle 1/\sigma \rangle$ and plasma nonuniformity factor $G = g + (g-1)\beta^2$ are lower limits based on two-dimensional calculations. In view of the asymmetric heat transfer in this channel, it is quite possible that the value of g is higher than 1.03, in which case the estimated conductivity is higher. For example, if $g = 1.2$, then conductivity becomes 114 S/m. At a lower limit, even if the Hall parameter was zero, the conductivity would be 89 S/m.

During self-excitation, the reactive component of the magnet impedance varies, and the generator operates over a range of load factors. Because the characteristic gasdynamic times are two orders of magnitude shorter than the self-excitation time constant, the self-excitation process can be viewed as a sequence of quasisteady generator states in which the flowfield is in equilibrium with the slower electrical circuit parameters. Figure 12 presents a simulated steady or quasisteady voltage/current characteristic for the self-excited generator with conditions typical of test 84-004. The generator traverses such a characteristic during self-excitation.

Because the self-excitation process is quasisteady, the generator load line traversed during self-excitation is similar to its load line at steady state if the combustor conditions are similar as well. Thus the load resistance for maximum power at steady state can be inferred from the reactive component of the magnet impedance at peak generator power during self-excitation. For example, at peak power in test 84-004, the reactive component of the magnet impedance was about 44 m Ω , and the 67-m Ω load inserted after switch S2 opened was apparently too high for maximum steady-state power.

The above arguments are valid when the generator performance exhibits no hysteresis. That is, when the instantaneous generator performance is not determined by the flow history but merely by the instantaneous operating conditions. Such is not necessarily the case in the presence of large flow disturbances or current concentrations created by magneto-aerothermal effects.

Field Distributions

The voltage distributions obtained in this generator are quite regular, particularly when compared with some other diagonal generator data. Figure 13 illustrates the measured voltages at two times in test 84-002. During self-excitation the slope of the voltage curve increases from front to rear. This indicates a rising Hall field associated with the accelerating flow shown by the simulations in Figs. 10 and 11.

After self-excitation is complete, the slope of the voltage curve drops at frame 6, indicating a discontinuity in the Hall field at that station. When the frame voltage data are differentiated, temporally smoothed with an 11-point moving average, and displayed on an $x-t$ diagram (Fig. 14), it becomes clear that the discontinuity starts at the back of the generator and moves forward as the load current increases.

One may speculate on the causes of this Hall field discontinuity. The quasi-one-dimensional simulation does not predict a shock so far upstream. A likely possibility is that it is behavior similar to the Hall field depression in the rear of the AEDC/HPDE during run 007-016, which was associated with the magnetoaerothermal current constriction and flow separation on the anode wall. Three-dimensional simulations would help resolve the operative mechanisms.

The graphite frame resistance is typically 1-2 m Ω from anode to cathode. The ballasting effect of this resistance¹² promotes the electric field uniformity exhibited in Figs. 13 and 14. Joule dissipation in the frames is estimated to amount to 1.8% of the gross power generated in test 84-004. It is possible to estimate the generator current densities within 5-10% on the basis of the frame voltage difference from anode to cathode and a measured frame resistance. Figure 15 presents results obtained in this way at various times in test 84-004. It is clear that the net Hall current density is substantial and that its direction changes during the test.

It has been shown in Refs. 13 and 14 that even moderate Hall current densities can have a profound influence on the flow distribution in an MHD generator. Girshick and Kruger^{15,16} have recently made careful measurements of these effects at Hall current densities up to 0.8 A/cm^2 , and the results appear to be in satisfactory agreement with the predictions of the STD/MHD codes.¹⁴ Fully three-dimensional calculations with validated STD/MHD codes¹⁷⁻¹⁹ have not been carried out for the Hall current densities of 10 A/cm^2 possible in the present device.

One manifestation of the magnetoaerothermal effect is a pronounced asymmetry in heat flux to the anode and cathode walls. The present device exhibits such asymmetries (Fig. 16).

Interaction Parameters

Recent work¹³ has shown that to simulate experimentally some important magnetoaerothermal effects, such as the anode current constriction in the AEDC/HPDE,^{20,21} it is not sufficient to create strong secondary flows by matching the interaction parameter based on velocity. The pressure interaction parameter also plays a crucial role by ensuring that there is sufficient current density and Joule dissipation to constrict and sustain the anode discharge when secondary flows create the necessary conditions. In general, flow behavior scales with the velocity interaction parameter, while performance scales with the pressure interaction parameter. Both appear important in scaling nonideal processes such as the magnetoaero thermal current constriction.²²

It is noted that the interaction parameter based on pressure, $I_p = \langle J_y B/p \rangle L$, exceeds 2 in the present device. This level of pressure interaction is roughly that required in large-scale utility MHD plants.¹¹ The comparable I_p is estimated to be 1.4 for the AEDC/HPDE, 1.6 for a 200-500-MW coal-fired utility generator, and 2 for the Pamir-I. The velocity interaction parameter in the present device is comparable to the AEDC/HPDE values $S_u = 2$.¹³

Conclusion

The diagonal generator has been shown to be an effective configuration for self-excited MHD generators with sufficient electrical conductivity in the working fluid. Superior self-excitation times have been achieved in a lightweight system.

The generator tests to date exhibit anomalous behavior in the electric field and heat flux distributions and in the wall erosion in the diffuser. These anomalies are strongly suggestive of the magnetoaerothermal current constriction/anode boundary-layer separation observed in AEDC/HPDE. On the other hand, no remarkable damage has occurred on the electrodes in the generator tests to date.

While there are many straightforward steps that may be taken to improve upon the initial performance of the present device (e.g., greater expansion ratio), achievement of the highest levels of enthalpy extraction will require detailed understanding and exploitation of the flow processes in high-interaction MHD devices operating with a controllable level of Hall current.

Acknowledgments

This experimental work was sponsored in part by the U.S. Navy, Naval Surface Weapons Center, Dahlgren, Virginia, under Contract N60921-84-C-A069 and earlier contracts. The authors are grateful to Drs. Bob DeWitt and Frank Rose for their support and encouragement. High-interaction MHD simulations of the experiments were carried out in part with the support of the U.S. Air Force Office of Scientific Research under Contract F49620-84-C-0068 under the direction of Majors Henry Pugh and Bruce Smith. Contributions to the hardware development by Mr. C. D. Bangert and to the theory of the generator system by Dr. D.A. Oliver are gratefully acknowledged. Thanks are due also to technicians J. P. Superata and C.H. Deichler, who started working with S. T.

Demetriades in 1959 and 1966, respectively. These results were first presented in a paper with the same title given at the 23rd Symposium on Engineering Aspects of Magnetohydrodynamics.²³

References

- ¹Mattsson, A.C.J., Ducharme, E.L., Govoni, E.M., Morrow, I.B. Jr., and Brogan, T.R., "Magnetohydrodynamic Power," *Mechanical Engineering*, Vol. 88, Nov. 1966, pp. 38-41.
- ²Rudins, G. et al., "A Study of the Operation of the U-25B Facility MHD Generator Under Conditions of Strong Electric and Magnetic Fields," *Proceedings of the Seventh International Conference on MHD Electrical Power Generation*, MIT, Cambridge, MA, 1980, pp. 1-11.
- ³Velikhov, E.P., Volkov, Y.M., Zotov, A.V., Matveenkov, O.G., and Yakushev, A.A., "Investigation of Factors Affecting the Self-excitation of Pulsed MHD Generators," *Proceedings of the Sixth International Conference on MHD Electrical Power Generation*, Washington, D.C., 1975.
- ⁴Holzman, A.L. and Burchard, J.K., "Hybrid MHD Plasma Sources," *Proceedings of the Ninth Symposium on Engineering Aspects of Magnetohydrodynamics*, University of Tennessee Space Institute, Tullahoma, TN, April 1968.
- ⁵Breev, V.V., Gubarev, A.V., Laptev, S.A., and Panchenko, V.P., "Transients in the Load Circuit of a Self-Excited MHD Generator, and Optimization of Its Parameters," *Proceedings of the Eighth International Conference on MHD Electrical Power Generation*, U.S.S.R. Academy of Science, Moscow, Sept. 1983.
- ⁶Doperchuk, I.I. and Konev, S.M.-A., "Self-Excitation of a Diagonal MHD Channel," *Magnitnaya Gidrodinamika*, No. 1, Jan.-March 1982, pp. 117-124.
- ⁷Demetriades, S.T., Oliver, D.A., Swean, T.F. Jr., and Maxwell, C.D., "On the Magnetoaerothermal Instability," AIAA Paper 81-0248, Jan. 1981.
- ⁸Kessler, R., Sonju, O.K., Teno, J., Lontai, L., and Meader, D., "MHD Power Generation (Viking Series) with Hydrocarbon Fuels," Avco Everett Research Laboratory, Final Technical Rept. AFAPL-TR-74-47, Part III, Nov. 1974.
- ⁹Demetriades, S.T., "Experimental Magnetogasdynamics Engine for Argon, Nitrogen and Air," Norair Division, Northrop Corp., ASRL TM-60-63, Nov. 1980; also *Engineering Aspects of Magnetohydrodynamics*, Proceedings of the 2nd EAM Symposium, Columbia University Press, 1962, pp. 19-44.
- ¹⁰Oliver, D.A., Crouse, R.D., Maxwell, C.D., and Demetriades, S.T., "Transient Response of Large Experimental MHD Power Generator Flowtrain Systems," AIAA Paper 80-0025, Jan. 1980.
- ¹¹Maxwell, C.D., Demetriades, S.T., Oliver, D.A., Vetter, A.A., and Swean, T.F. Jr., "Scale-up of Advanced MHD Generators," AIAA Paper 80-0179, Jan. 1980.
- ¹²Lowenstein, A. and Solbes, A., "Electrical Nonuniformities and Their Control in MHD Channels," *Proceedings of the 15th Symposium on Engineering Aspects of Magnetohydrodynamics*, The University of Pennsylvania, Philadelphia, PA, May 1976, pp. IX.3.1-IX.3.7..
- ¹³Maxwell, C.D., Demetriades, J.T., Oliver, D.A., and Demetriades, S.T., "Consideration of Optimum Boundary Configurations for Linear MHD Generators," *Proceedings of the 22nd Symposium on Engineering Aspects of Magnetohydrodynamics*, Mississippi State University, June 1984, pp. 2:1:1-2:1:25.
- ¹⁴Maxwell, C.D., Early, D.W., and Demetriades, S.T., "Predicted Strength and Influence of MHD-Induced Secondary Flows in Recent Experiments," *Proceedings of the 23rd Symposium on Engineering Aspects of Magnetohydrodynamics*, Pittsburgh Energy Technology Center, Somerset, PA, June 1985, pp. 173-188.
- ¹⁵Girshick, S.L. and Kruger, C.H., "Measurements of Secondary Flow in an MHD Channel," *Proceedings of the 22nd Symposium on Engineering Aspects of Magnetohydrodynamics*, Mississippi State University, June 1984, pp. 2:7:1-2:7:17.
- ¹⁶Girshick, S.L. and Kruger, C.H., "Experimental Study of Secondary Flow in an MHD Channel," *Proceedings of the 23rd Symposium on Engineering Aspects of Magnetohydrodynamics*, Pittsburgh Energy Technology Center, Somerset, PA, June 1985, pp. 159-172.
- ¹⁷"Numerical Solution of the Coupled Three-Dimensional Magnetohydrodynamic Channel Problem," STD Research Corporation, Arcadia, CA, Final Rept. STD-75-001, Jan. 1975.

¹⁸"STD/MHD Code Descriptions for Computer Programs Utilized Under Contract AC-01-79-ET15501," STD Research Corporation, Arcadia, CA, Rept. STDR-79-3, Jan. 1979.

¹⁹"Brief Technical Discussion of the Consistent STD/MHD Code System," STD Research Corporation, Arcadia, CA, Rept. STDR-82-7, Feb. 1982.

²⁰Demetriades, S.T., Maxwell, C.D., and Oliver, D.A., "Progress in Analytical Modeling of MHD Power Generators, II," *Proceedings of the 21st Symposium on Engineering Aspects of Magnetohydrodynamics*, Argonne National Laboratory, Argonne IL, June 1983.

²¹Whitehead, G.L., Christensen, L.S., and Felderman, E.J., "MHD Performance Demonstration Experiment, Final Rept. FY 74

to FY 84," Arnold Engineering Development Center, Arnold AFS, TN, DOE/ET/11417-20, June 1984.

²²Demetriades, S.T. and Maxwell, C.D., "Devices with Strong MHD Interaction," *Proceedings of the 23rd Symposium on Engineering Aspects of Magnetohydrodynamics*, Pittsburgh Energy Technology Center, Somerset, PA, June 1985, pp. 193-212.

²³Maxwell, C.D. and Demetriades, S.T., "Initial Tests of a Lightweight Self-Excited MHD Power Generator," *Proceedings of the 23rd Symposium on Engineering Aspects of Magnetohydrodynamics*, Pittsburgh Energy Technology Center, Somerset, PA, June 1985, pp. 147-158.

From the AIAA Progress in Astronautics and Aeronautics Series . . .

TRANSONIC AERODYNAMICS—v. 81

Edited by David Nixon, Nielsen Engineering & Research, Inc.

Forty years ago in the early 1940s the advent of high-performance military aircraft that could reach transonic speeds in a dive led to a concentration of research effort, experimental and theoretical, in transonic flow. For a variety of reasons, fundamental progress was slow until the availability of large computers in the late 1960s initiated the present resurgence of interest in the topic. Since that time, prediction methods have developed rapidly and, together with the impetus given by the fuel shortage and the high cost of fuel to the evolution of energy-efficient aircraft, have led to major advances in the understanding of the physical nature of transonic flow. In spite of this growth in knowledge, no book has appeared that treats the advances of the past decade, even in the limited field of steady-state flows. A major feature of the present book is the balance in presentation between theory and numerical analyses on the one hand and the case studies of application to practical aerodynamic design problems in the aviation industry on the other.

Published in 1982, 669 pp., 6×9, illus., \$45.00 Mem., \$75.00 List

TO ORDER WRITE: Publications Dept., AIAA, 1633 Broadway, New York, N.Y. 10019